A Letters Journal Exploring the Frontiers of Physics

January 2015

EPL, **109** (2015) 10003
doi: 10.1209/0295-5075/109/10003

www.epljournal.org

Diffusion of chiral Janus particles in a sinusoidal channel

Xue Ao[1], P. K. Ghosh[2], Y. Li[3(a)], G. Schmid[1], P. Hänggi[1,3] and F. Marchesoni[3,4]

[1] *Institut für Physik, Universität Augsburg - D-86135 Augsburg, Germany*
[2] *Department of Chemistry, Presidency University - Kolkata, 700073, India*
[3] *Center for Phononics and Thermal Energy Science, School of Physics Sciences and Engineering, Tongji University Shanghai 200092, PRC*
[4] *Dipartimento di Fisica, Università di Camerino - I-62032 Camerino, Italy*

received 13 August 2014; accepted in final form 16 December 2014
published online 15 January 2015

PACS 05.40.Jc – Brownian motion
PACS 82.70.Dd – Colloids
PACS 87.15.hj – Transport dynamics

Abstract – We investigated the transport diffusivity of artificial microswimmers, a.k.a. Janus particles, in the absence of external biases. We considered the case of chiral Janus particles moving either in the bulk or in sinusoidal channels with reflecting walls. Their self-diffusion constants turned out to depend on both the strength and the chirality of the self-propulsion mechanism. More importantly, in a periodic channel self-diffusion can be controlled by tailoring the compartment geometry.

Introduction. – Over the last decade the problem of controlling transport of regular Brownian particles in narrow corrugated channels has attracted the attention of many investigators with the purpose of better understanding biological processes in the cell or designing artificial micro- and nano-devices [1,2]. In a recent development [3] regular Brownian particles have been replaced with a special type of diffusive tracers, namely, with active or self-propelled artificial microswimmers. Since such particles operate by harvesting energy from their environment, mostly in a nonequilibrium steady state, their autonomous transport is generally enhanced [3].

Self-propulsion is the ability of most living organisms to move, in the absence of external drives, thanks to an "engine" of their own [4]. Optimizing self-propulsion of micro- and nano-particles (artificial microswimmers) is a growing topic of today's nanotechnology [5–8]. In artificial microswimmers [9,10] self-propulsion takes advantage of the local gradients asymmetric particles can generate in the presence of an external energy source (self-phoretic effects). Such particles, called Janus particles (JP), consist of two distinct "faces", only one of which is chemically or physically active [11]. Thanks to their functional asymmetry, JP's can induce either concentration gradients (self-diffusiophoresis) by catalyzing a chemical reaction on their active surface [12–14], or thermal gradients (self-thermophoresis), *e.g.*, by inhomogeneous light absorption [15] or magnetic excitation [16].

The self-propulsion mechanism acting on an pointlike particle can be modeled in terms of an effective force and, possibly, an effective torque, which result from local gradients in the suspension fluid surrounding the particle. In contrast with the case of externally applied macroscopic gradients, such phoretic forces and torques cause no long-range flow patterns in the fluid; as we do not explicitly account for the fluid flow disturbances, phoretic forces and torques are taken here as independent model parameters (for more details see the discussion in ref. [17]). In the absence of a torque, the line of motion is directed parallel to the self-phoretic force and the JP propels itself along a straight line, until it changes direction after a mean persistence length, l_θ, due to gradient fluctuations [18] or random collisions against other particles or geometric boundaries [19]. In the presence of asymmetries in the propulsion mechanism, the self-phoretic force and the line of motion are no longer aligned and the microswimmer tends to execute circular orbits with radius R_Ω, as if subject to a torque with chiral frequency Ω [20,21] (fig. 1).

Active chiral motion has long been known in biology [21–23] and more recently observed in asymmetrically propelled micro- and nano-rods: A torque can be intrinsic to the propulsion mechanism, due to the presence of

(a) E-mail: yunyunli@tongji.edu.cn

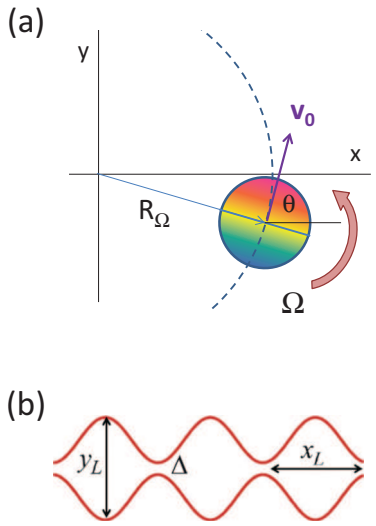

Fig. 1: (Color online) (a) Chiral levogyre Janus particle with $\Omega > 0$ in the bulk. Sketch of a noiseless particle with self-propulsion velocity $\mathbf{v}_0$ and finite torque frequency Ω, eq. (1), moving along a circular arc of radius R_Ω (dashed line); (b) Sketch of the sinusoidal channel of eq. (2). Due to its symmetry, this channel does not rectify JP diffusion.

geometrical asymmetries in the particle fabrication, engineered or accidental (asymmetric JP's) [24–26], or externally applied, for instance, by laser irradiation [15] or hydrodynamic fields [27].

Active Brownian motion is time correlated *per se*, which means that rectification of a JP can be easily achieved by choosing spatially asymmetric channel boundaries [3]. As we intend to investigate the interplay of propulsion chirality and geometric confinement on the diffusivity of a channeled JP, here we restrict our analysis to the case of sinusoidal channels, where the rectification current is known to be identically zero, both for passive and active Brownian motion. The extension of the present work to the case of spatially asymmetric channels will be presented elsewhere. The main results presented below can be summarized as follows: i) A finite torque, $|\Omega| > 0$, tends to suppress the particle diffusivity even in the bulk, according to a simple law that fits remarkably well the simulation data. This effect grows prominent for chiral radii much shorter than the self-propulsion length, $R_\Omega \ll l_\theta$. ii) The diffusivity of channeled microswimmers, besides decreasing with $|\Omega|$ as in the bulk, exhibits an additional side peak, which corresponds to the optimal condition, when a channel compartment can accommodate for a closed orbit of the chiral swimmer, thus trapping it. iii) These properties are rather sensitive to both the self-propulsion mechanism of the microswimmer and the geometry of the channel, which points to simple techniques for sorting out microswimmers according to their swimming properties.

Model. – In order to avoid unessential complications, we restrict our analysis to the case of 2D channels and pointlike artificial microswimmers of the JP type [9]. The extension of our conclusions to 3D channels and finite-size particles [28] is straightforward. A chiral JP gets a continuous push from the suspension fluid, which in the overdamped regime amounts to a rotating self-propulsion velocity $\mathbf{v}_0$ with independent, constant modulus v_0 and angular velocity Ω. Additionally, the self-propulsion direction varies randomly with time constant τ_θ, under the combined action of thermal noise and orientational fluctuations intrinsic to the self-propulsion mechanism.

The bulk dynamics of such an overdamped chiral JP obeys the Langevin equations [20,23,29]

$$\begin{aligned} \dot{x} &= v_0 \cos\theta + \xi_x(t), \\ \dot{y} &= v_0 \sin\theta + \xi_y(t), \\ \dot{\theta} &= \Omega + \xi_\theta(t), \end{aligned} \tag{1}$$

where the coordinates of the particle center of mass, $\mathbf{r} = (x, y)$, are subject to the Gaussian noises $\xi_i(t)$, with $\langle \xi_i(t) \rangle = 0$ and $\langle \xi_i(t)\xi_j(0) \rangle = 2D_0\delta_{ij}\delta(t)$ for $i = x, y$, modeling the equilibrium thermal fluctuations in the suspension fluid. The channel is directed along the x-axis, the self-propulsion velocity is oriented at an angle θ with respect to it and the sign of Ω is chosen so as to coincide respectively with the positive (levogyre) and negative (dextrogyre) chirality of the swimmer, see fig. 1. The orientational fluctuations of the propulsion velocity are modeled by the independent Gaussian noise $\xi_\theta(t)$ with $\langle \xi_\theta(t) \rangle = 0$ and $\langle \xi_\theta(t)\xi_\theta(0) \rangle = 2D_\theta\delta(t)$, where, as shown below, D_θ sets the orientational time constant, τ_θ, of the self-propulsion velocity, $\tau_\theta = 2/D_\theta$. Accordingly, the microswimmer mean free self-propulsion path approximates a circular arc of radius $R_\Omega = v_0/|\Omega|$ and length $l_\theta = v_0\tau_\theta$ [20]. Therefore, for $R_\Omega \lesssim l_\theta$, or equivalently, $|\Omega|\tau_\theta \gtrsim 1$ (strong chirality regime), chiral effects tend to appreciably suppress the ensuing active Brownian diffusion as shown below.

All noise sources in eq. (1) have been treated as independently tunable, although, strictly speaking, thermal and orientational fluctuations may be statistically correlated depending on the self-propulsion mechanism [5,12,14]. Moreover, we ignored hydrodynamic effects, which are known to favor clustering in dense mixtures of JP's [30,31] and even cause their capture by the channel walls [32], and the possible effects of a reflecting obstacle on the JP self-propulsion mechanism. However, both effects are mitigated by considering low density mixtures of pointlike spherical JP's. Moreover, we made sure that the parameters used in our simulations were experimentally accessible, as apparent on expressing times in seconds and lengths in microns and comparing with the experimental setups of refs. [14,23].

When confined to a channel directed along the x-axis, the particle transverse coordinate, y, is bounded between a lower and upper wall, $w_-(x) \le y \le w_+(x)$, with

$$w_\pm(x) = \pm\frac{1}{2}\left[\Delta + (y_L - \Delta)\sin^2\left(\frac{\pi}{x_L}x\right)\right]. \tag{2}$$

Such a sinusoidal channel is periodic; its compartments have length x_L and are mirror symmetric under both coordinate inversions, $x \to -x$ and $y \to -y$, *i.e.*, centrosymmetric. Throughout our analysis we assumed that the width, Δ, of the pores connecting the compartments are much narrower than the maximum channel cross-section, *i.e.*, $\Delta \ll y_L$.

Simulating a constrained JP requires defining its collisional dynamics at the boundaries. For the translational velocity $\dot{\mathbf{r}}$ we assumed elastic reflection. Regarding the coordinate θ, we assumed that it does not change upon collision (sliding b.c. [3]). As a consequence the active particle slides along the walls for an average time of the order of τ_θ, until the θ fluctuations, $\xi_\theta(t)$, redirect it toward the interior of the compartment. The present b.c. choice is consistent with reported experimental observations [14], though, as mentioned above [32], not universal (see also [33]). Different b.c. do not change the qualitative picture emerging from our investigation [3]: For strongly persistent propulsion mechanisms, $l_\theta \gg x_L, y_L$, and weak chirality, $R_\Omega \gg l_\theta$, the stationary particle probability density $P(x,y)$ accumulates along the boundaries; this effect is the strongest in the noiseless case, $D_0 = 0$.

The dispersion of a Brownian particle along the channel axis [34] is an important issue experimentalists address when trying to demonstrate rectification. Indeed, drift currents, no matter how weak, can be detected over an affordable observation time only if the relevant dispersion is sufficiently small. This issue is of paramount importance when one handles with active Brownian particles, like JP', whose stochastic dynamics is characterized by strong persistency, or long correlation times. Under such conditions the current literature on classical diffusion is of little help [1,35]. To this purpose we computed the transport diffusivity, $D_{\rm ch}$, of a JP in the sinusoidal channel of eq. (2), as the limit

$$D_{\rm ch} = \lim_{t\to\infty} [\langle x^2(t)\rangle - \langle x(t)\rangle^2]/(2t), \tag{3}$$

which we checked to exist for all simulation parameters (normal diffusion limit).

Bulk diffusion, D**.** – A full analytical solution of the model eq. (1) is cumbersome even in the bulk (*i.e.*, in the absence of boundaries). However, the particle mean square displacement can be easily computed by noticing that

$$\begin{aligned}\langle \cos\theta(t)\cos\theta(0)\rangle &= \langle \sin\theta(t)\sin\theta(0)\rangle \\ &= (1/2)\cos(\Omega t)e^{-D_\theta|t|},\end{aligned} \tag{4}$$

and the first two LEs of eq. (1) are statistically independent, namely $\lim_{t\to\infty}\langle\cos\theta(t)\sin\theta(t)\rangle = 0$. It follows immediately that a *nonchiral* particle ($\Omega = 0$) diffuses according to Fürth's law [36]

$$\begin{aligned}\langle \Delta x(t)^2\rangle &= \langle \Delta y(t)^2\rangle \\ &= 2(D_0 + v_0^2\tau_\theta/4)t + (v_0^2\tau_\theta^2/2)(e^{-2t/\tau_\theta} - 1).\end{aligned} \tag{5}$$

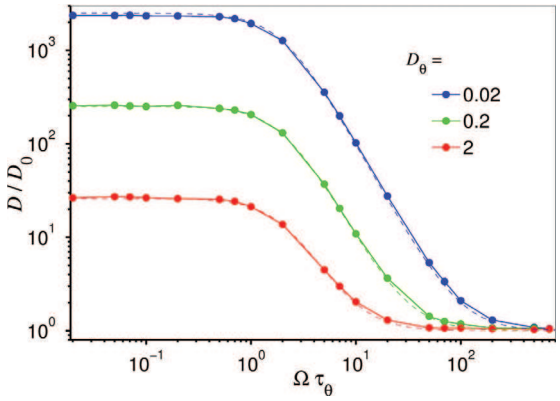

Fig. 2: (Color online) Diffusion of a levogyre JP with $\Omega \geq 0$ and $v_0 = 1$ in a straight channel: $D_{\rm ch}$ *vs.* Ω for different D_θ and $D_0 = 0.01$. The boundaries $w_\pm(x)$ are given by eq. (2) with $\Delta = y_L = 1$. The dashed curves represent the corresponding phenomenological law, $D_{\rm ch} = D$, holding for straight channels, with D given in eq. (8). Our results are independent of the sign of Ω and the width of the straight channel (not shown).

For $t \gg \tau_\theta$ we thus recover the asymptotic normal diffusion law, $\langle \Delta x(t)^2\rangle = 2Dt$, where the constant D apparently consists of two distinct contributions,

$$D = D_0 + D_s, \tag{6}$$

due to the randomness of, respectively, the thermal fluctuations, D_0, and self-propulsion, $D_s = v_0^2\tau_\theta/4$ (self-diffusivity).

Determining the Ω dependence of the bulk diffusivity, $D(\Omega)$, of a *chiral* JP requires more laborious algebraic passages. Eventually, eq. (5) is replaced by [20,37–39]

$$\begin{aligned}&\langle \Delta x(t)^2\rangle = \langle \Delta y(t)^2\rangle = 2D_0 t \\ &+ v_0^2\left[\frac{D_\theta}{D_\theta^2+\Omega^2}t + \frac{D_\theta^2-\Omega^2}{(D_\theta^2+\Omega^2)^2}(e^{-D_\theta t}\cos\Omega t - 1)\right] \\ &- 2v_0^2\frac{D_\theta\Omega}{(D_\theta^2+\Omega^2)^2}e^{-D_\theta t}\sin\Omega t,\end{aligned} \tag{7}$$

and, accordingly, the bulk diffusivity becomes

$$D(\Omega) = D_0 + \frac{D_s}{1+(\Omega\tau_\theta/2)^2}, \tag{8}$$

where $D(0)$ coincides with D in eq. (3). In conclusion, chirality tends to suppress the self-diffusivity of a Janus particle.

Owing to the b.c. adopted here, for a JP diffusing in a straight channel, say, with $w_\pm(x) = \pm y_L/2$, bulk and channel diffusivity coincide, $D_{\rm ch} = D$. This statement is confirmed by the fact that the simulation curves displayed in fig. 2 do not depend on y_L. Most remarkably, all three curves are closely fitted by the phenomenological law (8). As expected from eq. (8), $D(\Omega)$ interpolates the diffusivity of a nonchiral JP, eq. (6), at $\Omega = 0$ and the thermal diffusivity, D_0, for $\Omega \to \infty$. In the latter limit, *i.e.*, for $R_\Omega/l_\theta \to 0$, diffusion from self-propulsion is totally suppressed.

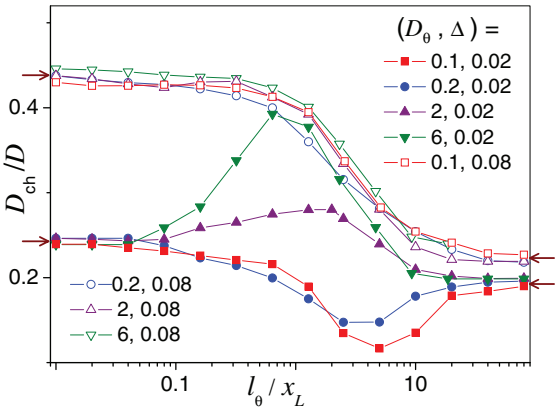

Fig. 3: (Color online) Diffusion of a nonchiral JP in the sinusoidal channel of eq. (2): $D_{\rm ch}/D$ *vs.* v_0 at constant D_θ and Δ (see legend). D is the bulk diffusivity of eq. (6). Other simulation parameters are $x_L = y_L = 1$ and $D_0 = 0.05$. The left and right arrows denote, respectively, the estimated values of the suppression constants, κ_0 and κ_s, introduced in the text, *i.e.*, $\kappa_0 = 0.25$ and $\kappa_s = 0.20$ for $\Delta = 0.02$; $\kappa_0 = 0.45$ and $\kappa_s = 0.23$ for $\Delta = 0.08$.

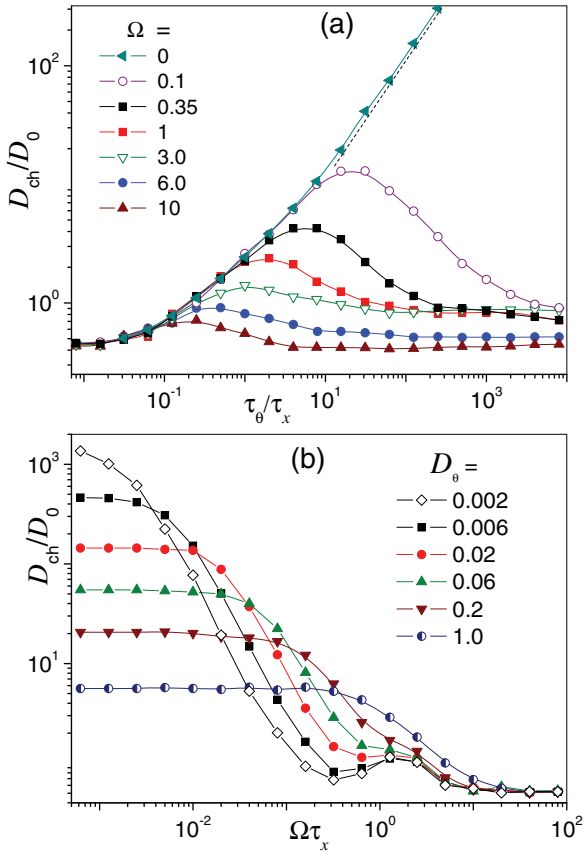

Fig. 4: (Color online) (a) Diffusion of a levogyre JP in the sinusoidal channel of eq. (2): (a) $D_{\rm ch}/D_0$ *vs.* τ_θ for different Ω. Notice that the smaller Ω, the slower is the convergence of $D_{\rm ch}/D_0$ to κ_0 for large τ_θ. (b) $D_{\rm ch}/D_0$ *vs.* Ω for different D_θ. Here, $\tau_x = x_L/v_0$, $v_0 = 1$, $D_0 = 0.05$, and $\Delta = 0.08$. The dashed line in (a) represents the asymptotic linear power law of eq. (6).

Channel diffusion, $D_{\rm ch}$. – When confined to a corrugated channel, the particle diffusivity is suppressed by the geometric constrictions represented by the pores, as shown in figs. 3 and 4, respectively, for nonchiral and chiral JP's diffusing along a sinusoidal channel.

In the absence of self-propulsion, say, for $v_0 = 0$ (or, equivalently, $l_\theta = 0$), the bulk diffusivity is $D = D_0$, see eq. (6), and the channel diffusivity can be written as $D_{\rm ch} = \kappa_0 D_0$, with κ_0 a well-studied function of Δ and D_0 [40,41]. In the opposite limit, $v_0 \to \infty$, the bulk diffusion of a *nonchiral* JP is governed by self-propulsion, that is, $D \simeq D_s$ and, accordingly, in the channel $D_{\rm ch} = \kappa_s D_s$. Both limits of $D_{\rm ch}$ are illustrated in fig. 3 for different values of Δ and D_θ. Apparently, neither κ_0 nor κ_s depend on D_θ and both are smaller than one. This conclusion applies to different compartment geometries, symmetric and asymmetric, alike, as confirmed by further simulation results not reported here.

The mechanisms underlying the suppression of channel diffusion quantified by the constants κ_0 and κ_s, are different. For a regular Brownian particle with $v_0 = 0$ moving in a narrow channel, κ_0 can be estimated in Fick-Jacobs' approximation for smoothly corrugated channels [1,40] and in mean-first-exit time formalism for sharply compartmentalized channels [41,42]. In both cases, κ_0 strongly depends on the compartment volume, the pore width and thermal noise, since particle diffusion mostly happens away from the walls. For nonchiral self-propelling microswimmers with $l_\theta \gg x_L, y_L$, the constant κ_s is mostly determined by the b.c. introduced to model the particle collisions against the channel walls. For sliding b.c., the probability flows (consequence of the JP's piling up against the boundaries [29]) are modulated by the wall profiles, $w_\pm(x)$, and thus not much sensitive to the pore width itself (as long as the particle size is negligible). The distinct Δ dependence of κ_0 and κ_s is apparent in fig. 3.

We consider next the case of channeled *chiral* JP's. The diffusivity of a levogyre JP's in a sinusoidal channel, illustrated in fig. 4, clearly points to two different chirality-induced suppression mechanisms. We have already shown how chirality limits the bulk the diffusion of JP's with long self-propulsion time constants, that is $|\Omega|\tau_\theta \gg 1$ or $R_\Omega \ll l_\theta$, see eq. (8). On the other hand, when the chiral radius R_Ω grows smaller than the compartment dimensions, say, $R_\Omega \ll x_L$, or the chiral frequency larger than the reciprocal of compartment crossing time, $\tau_x = x_L/v_0$, that is $|\Omega|\tau_x \gg 1$, all swimmers, even those with long self-propulsion length, $l_\theta \gg x_L$, are expected to perform closed orbits and thus get trapped inside the channel compartments [29]. Such a geometric condition is likely to produce an additional suppression of channel diffusion.

With these premises the dependence of $D_{\rm ch}$ on the self-propulsion mechanism parameters, τ_θ and Ω, can be satisfactorily explained, at least, at a qualitative level. Curves

of $D_{\rm ch}$ *vs.* τ_θ at constant Ω are reported in fig. 4(a). By inspection one notices immediately that: i) At large τ_θ, D_0 is negligible with respect to D_s and, again, $D_{\rm ch} \simeq \kappa_s D(\Omega)$, like for nonchiral JP's. Most remarkably, we checked that κ_s does not sensibly depend on Ω. ii) The curves $D_{\rm ch}$ *vs.* τ_θ go through a maximum, $D_{\rm ch}^{\rm max} \simeq \kappa_s D_s/2$, the position of which, $|\Omega|\tau_\theta = 2$, is insensitive to the channel geometry. Indeed, position and height of the maxima located at $\tau_\theta > \tau_x$ can be closely approximated by plotting the bulk diffusivity of eq. (6) as a function of τ_θ and making use of the relation $D_{\rm ch} = \kappa_s D$. iii) For finite Ω, active diffusivity in the channel is suppressed both for $\tau_\theta \to 0$ and $\tau_\theta \to \infty$. In both limits, one thus expects that $D_{\rm ch}(\Omega) \to \kappa_0 D_0$, where κ_0 is the corresponding suppression constant at $\Omega = 0$ given in fig. 3. Note that at low Ω the convergence toward the expected large τ_θ asymptote is very slow. The same asymptote is approached by the large Ω tails of the curves plotted in fig. 4(b). The Ω dependence of $D_{\rm ch}$ at constant τ_θ, illustrated in fig. 4(b), shows explicitly that iv) $D_{\rm ch}$ starts decreasing appreciably with Ω only for $|\Omega|\tau_\theta \gtrsim 2$, that is in coincidence with the maxima displayed in fig. 4(a). v) Small diffusivity peaks emerge for $|\Omega|\tau_\theta \gg 1$. They are centered around a certain value of Ω, Ω_M, which does not depend on the time constant τ_θ. Ω_M can be estimated by noticing that on increasing Ω the chiral radius $R_\Omega = v_0/|\Omega|$ decreases, until the microswimmer performs a full circular orbit inside the channel compartment, without touching its walls (actually a logarithmic spiral with exponentially small steps [20]). In the noiseless limit, this happens for $2R_\Omega \simeq x_L$, that is, $\Omega_M \simeq 2v_0/x_L$. This condition can be regarded as the onset of a mechanism of dynamical trapping. In Brownian transport theory, the onset of a trapping mechanism generally corresponds to an excess diffusion peak [43–45]: That is precisely the phenomenon we see at work here. Of course, this argument requires that $\Omega_M \tau_\theta \gg 1$, to ensure a sufficiently long self-propulsion time. Both our estimate for Ω_M and the condition for the diffusivity peak to appear are in close agreement with the data displayed in fig. 4(b).

Conclusions. – We numerically investigated the diffusion of artificial active microswimmers moving along narrow periodically corrugated channels. Our work is meant to foster research on the rectification of active microswimmers in confined geometries. Transport quantifiers, like rectification power and diffusivity, strongly depend on the particle self-propulsion mechanism and the channel compartment geometry. The emerging picture suggests the possibility of developing new control techniques for the manipulation of artificial microswimmers, which are well within the reach of today's technology. Specialized microfluidic circuits can be designed, for instance, to guide chiral microswimmers to a designated target. The same technique can be utilized to fabricate monodisperse chiral microswimmers (presently a challenging technological task). By the same token, microswimmers capable of inverting chirality upon binding to a load, can operate as chiral shuttles along a suitably corrugated channel even in the absence of gradients of any kind.

* * *

XA has been supported by the grant Equal Opportunity for Women in Research and Teaching of the Augsburg University. PH and GS acknowledge support from the cluster of excellence Nanosystems Initiative Munich (NIM). YL was supported by the NSF China under grants No. 11347216 and 11334007, and by Tongji University under grant No. 2013KJ025. FM thanks the Alexander von Humboldt Stiftung for a Research Award.

REFERENCES

[1] Burada P. S., Hänggi P., Marchesoni F., Schmid G. and Talkner P., *ChemPhysChem*, **10** (2009) 45.
[2] Hänggi P. and Marchesoni F., *Rev. Mod. Phys.*, **81** (2009) 387.
[3] Ghosh P. K., Misko V. R., Marchesoni F. and Nori F., *Phys. Rev. Lett.*, **110** (2013) 268301.
[4] Purcell E. M., *Am. J. Phys.*, **45** (1977) 3.
[5] Schweitzer F., *Brownian Agents and Active Particles* (Springer, Berlin, Heidelberg) 2003.
[6] Ramaswamy S., *Annu. Rev. Condens. Matter Phys.*, **1** (2010) 323.
[7] Vicsek T. and Zafeiris A., *Phys. Rep.*, **517** (2012) 71.
[8] Romanczuk P., Bär M., Ebeling W., Lindner B. and Schimansky-Geier L., *Eur. Phys. J. ST*, **202** (2012) 1.
[9] Jiang S. and Granick S. (Editors), *Janus Particle Synthesis, Self-Assembly and Applications* (RSC Publishing, Cambridge) 2012.
[10] Walther A. and Müller A. H. E., *Chem. Rev.*, **113** (2013) 5194.
[11] Golestanian R., Liverpool T. B. and Ajdari A., *New J. Phys.*, **9** (2007) 126.
[12] Paxton W. F., Sundararajan S., Mallouk T. E. and Sen A., *Angew. Chem., Int. Ed.*, **45** (2006) 5420.
[13] Howse J. R., Jones R. A. L., Ryan A. J., Gough T., Vafabakhsh R. and Golestanian R., *Phys. Rev. Lett.*, **99** (2007) 048102.
[14] Volpe G., Buttinoni I., Vogt D., Kümmerer H.-J. and Bechinger C., *Soft Matter*, **7** (2011) 8810.
[15] Jiang H. R., Yoshinaga N. and Sano M., *Phys. Rev. Lett.*, **105** (2010) 268302.
[16] Baraban L., Streubel R., Makarov D., Han L., Karnaushenko D., Schmidt O. G. and Cuniberti G., *ACS Nano*, **7** (2013) 1360.
[17] Felderhof B. U., *Phys. Rev. Lett.*, **113** (2014) 029801; Kümmel F., ten Hagen B., Wittkowski R., Buttinoni I., Eichhorn R., Volpe G., Löwen H. and Bechinger C., *Phys. Rev. Lett.*, **113** (2014) 029802; ten Hagen B., Wittkowski R., Takagi D., Kümmel F., Bechinger C. and Löwen H., arXiv:1410.6707v1.
[18] Hong Y., Velegol D., Chaturvedi N. and Sen A., *Phys. Chem. Chem. Phys.*, **12** (2010) 1823.

[19] Búzás A., Kelemen L., Mathesz A., Oroszi L., Vizsnyiczai G., Vicsek T. and Ormos P., *Appl. Phys. Lett.*, **101** (2012) 041111.
[20] van Teeffelen S. and Löwen H., *Phys. Rev. E*, **78** (2008) 020101.
[21] Friedrich B. M. and Jülicher F., *Phys. Rev. Lett.*, **103** (2009) 068102.
[22] Brokaw C. J., *J. Exp. Biol.*, **35** (1958) 97; *J. Cell. Comp. Physiol.*, **54** (1959) 95.
[23] Mijalkov M. and Volpe G., *Soft Matter*, **9** (2013) 6376.
[24] Kümmel F., ten Hagen B., Wittkowski R., Buttinoni I., Eichhorn R., Volpe G., Löwen H. and Bechinger C., *Phys. Rev. Lett.*, **110** (2013) 198302.
[25] Boymelgreen A., Yossifon G., Park S. and Miloh T., *Phys. Rev. E*, **89** (2014) 011003(R).
[26] Sen A., Ibele M., Hong Y. and Velegol D., *Faraday Discuss.*, **143** (2009) 15.
[27] Zöttl A. and Stark H., *Phys. Rev. Lett.*, **108** (2012) 218104.
[28] Ten Hagen B., van Teeffelen S. and Löwen H., *J. Phys.: Condens. Matter*, **23** (2011) 194119.
[29] Li Y., Ghosh P. K., Marchesoni F. and Li B., *Phys. Rev. E*, **90** (2014) 062301; Ao X., Ghosh P. K., Li Y., Schmid G., Hänggi P. and Marchesoni F., *Eur. Phys. J. ST*, **223** (2014) 3227.
[30] Ripoll M., Holmqvist P., Winkler R. G., Gompper G., Dhont J. K. G. and Lettinga M. P., *Phys. Rev. Lett.*, **101** (2008) 168302.
[31] Buttinoni I., Bialkè J., Kümmel F., Löwen H., Bechinger C. and Speck T., *Phys. Rev. Lett.*, **110** (2013) 238301.
[32] Takagi D., Palacci J., Braunschweig A. B., Shelley M. J. and Zhang J., *Soft Matter*, **10** (2014) 1784.
[33] Zschiegner S., Russ S., Valiullin R., Coppens M.-O., Dammers A. J., Bunde A. and Kärger J., *Eur. Phys. J. ST*, **161** (2008) 109.
[34] Machura L., Kostur M., Talkner P., Luczka J., Marchesoni F. and Hänggi P., *Phys. Rev. E*, **70** (2004) 061105.
[35] Brenner H. and Edwards D. A., *Macrotransport Processes* (Butterworth-Heinemann, New York) 1993.
[36] Fürth R., *Z. Phys.*, **2** (1920) 2.
[37] Ebbens S., Jones R. A. L., Ryan A. J., Golestanian R. and Howse J. R., *Phys. Rev. E*, **82** (2010) 015304.
[38] Marine N. A., Wheat P. M., Ault J. and Posner J. D., *Phys. Rev. E*, **87** (2013) 052305.
[39] Nourhani A., Lammert P. E., Borhan A. and Crespi V. H., *Phys. Rev. E*, **87** (2013) 050301.
[40] Burada P. S., Schmid G., Reguera D., Rubi J. M. and Hänggi P., *Phys. Rev. E*, **75** (2007) 051111.
[41] Bosi L., Ghosh P. K. and Marchesoni F., *J. Chem. Phys.*, **137** (2012) 174110.
[42] Borromeo M. and Marchesoni F., *Chem. Phys.*, **375** (2010) 536.
[43] Schreier M., Hänggi P. and Pollak E., *Europhys. Lett.*, **44** (1998) 416.
[44] Costantini G. and Marchesoni F., *Europhys. Lett.*, **48** (1999) 491.
[45] Reimann P., Van den Broek C., Linke H., Hänggi P., Rubí J. M. and Perez Madrid A., *Phys. Rev. Lett.*, **87** (2001) 010602.